Buoyancy-Driven Flow Excursions in Fuel Assemblies (U)

CONF-950904 --1-Rev.

by

J. E. Laurinat

Westinghouse Savannah River Company
Savannah River Site
Aiken, South Carolina 29808

P. K. Paul
Westinghouse Savannah River Company
SC USA

J. D. Menna
Westinghouse Savannah River Company
SC USA

DISCLAIMER

DISCLAIMER

Portions of this document may be illegible in electronic image products. Images are produced from the best available original document.

BUOYANCY-DRIVEN FLOW EXCURSIONS
IN FUEL ASSEMBLIES (U)

James E. Laurinat
Pran K. Paul
John D. Menna

Westinghouse Savannah River Company
Savannah River Technology Center
Aiken, SC 29802

Abstract

A power limit criterion was developed for a postulated Loss of Pumping Accident (LOPA) in one of the recently shut down heavy water production reactors at the Savannah River Site. These reactors were cooled by recirculating heavy water moderator downward through channels in cylindrical fuel tubes. Powers were limited to safeguard against a flow excursion in one or more of these parallel channels.

During full-power operation, limits safeguarded against a boiling flow excursion. At low flow rates, during the addition of emergency cooling water, buoyant forces reverse the flow in one of the coolant channels before boiling occurs. As power increases beyond the point of flow reversal, the maximum wall temperature approaches the fluid saturation temperature, and a thermal excursion occurs.

The power limit criterion for low flow rates was the onset of flow reversal. To determine conditions for flow reversal, tests were performed in a mock-up of a fuel assembly that contained two electrically heated concentric tubes surrounded by three flow channels. These tests were modeled using a finite difference thermal-hydraulic code. According to code calculations, flow reversed in the outer flow channel before the maximum wall temperature reached the local fluid saturation temperature. Thermal excursions occurred when the maximum wall temperature approximately equaled the saturation temperature.

For a postulated LOPA, the flow reversal criterion for emergency cooling water addition was more limiting than the boiling excursion criterion for full power operation. This criterion limited powers to 37% of the limiting power for previous long-term reactor operations.

Background

The production reactors at the Savannah River Site had several unique features that dictated a different approach to power limits analysis than is commonly used for commercial power reactors. The Savannah River reactors used heavy water as a moderator and coolant and operated at much lower temperatures and pressures than commercial reactors. In contrast with boiling water reactors, external heat exchangers connected to local surface water sources maintained core temperatures below the boiling point, so these reactors did not generate any steam. The Savannah River reactors also differed from commercial reactors in that the coolant was recirculated downward rather than upward through the fuel tubes. Because of their relatively low core pressures and the downward flow through the fuel tubes, the Savannah River reactors were much more

susceptible to parallel channel, bulk boiling flow instabilities than are commercial reactors.

Commercial reactor powers commonly are limited to avoid a critical heat flux on one of the fuel element surfaces or a dryout of the liquid film on a heated surface. By contrast, power limits for the Savannah River reactors were set to safeguard against a parallel channel, bulk boiling flow instability during a postulated design-basis Loss of Coolant Accident (LOCA) [1]. In the LOCA, a line break in one of the lines to or from the external heat exchangers interrupts the supply of primary coolant, causing the reactor to scram. Power limits were set to prevent a parallel channel flow excursion during the two to three seconds immediately following the scram. This flow excursion occurs when the pressure drop reaches a minimum in one flow channel due to boiling in that channel. If the coolant flow rate decreases further, the boiling diverts flow to adjacent channels, so that the affected channel dries out and undergoes a thermal excursion. The limiting criterion for a boiling excursion was a lower bound [1] to the Saha-Zuber correlation for onset of significant void generation [2]. The lower bound to the Saha-Zuber correlation, which accounts for uncertainties in the correlation, takes the form of a Stanton number, given by

$$St = \frac{q''}{Gc_p(T_{sat} - T_{bulk})} = 0.0065 \tag{1}$$

By definition, the design-basis accident must be more limiting than other postulated accidents. One of these other accidents is the Loss of Pumping Accident (LOPA), in which a line break interrupts the supply of secondary cooling water to the heat exchangers. The secondary line break trips the power to the primary AC motors for the pumps that supply primary coolant. As a result, the primary pumps coast down and the coolant flow rate gradually drops, until the emergency cooling water supply is activated. This stabilizes the coolant flow rate until the backup DC pump motors become flooded with secondary cooling water. When these motors flood, the primary pumps eventually coast to a stop. A previous analysis indicated that the most limiting condition would probably occur during the coast down of the DC pump motors [3]. This analysis used a modified Stanton number criterion based on the results of flow excursion tests conducted in a single-channel test rig [4]:

$$St = 0.0025 \tag{2}$$

The purpose of this study was to generate a low flow power limit criterion based on results of flow excursion tests performed in a multiple-channel test rig [5]. This test rig, called SPRIHTE, or SRS Prototypic Rig for Heat Transfer Experiments, was operated by the Savannah River Site heat transfer test facility.

Description of Test Facility and Tests

The SPRIHTE test rig, depicted in Figure 1, was built to be prototypic of a Savannah River fuel assembly. The test rig was operated by recirculating ordinary light water downward through a heated section using a centrifugal pump. This heated section consisted of concentric heated tubes separated by spacer ribs. In two of the concentric tubes, electrical resistance heat was added through wires embedded between an aluminum base tube and a plasma-sprayed aluminum coating. The heat was removed by passing the coolant through a heat exchanger. As in the fuel assemblies, coolant entered and exited the test rig through perforations in the sides of the outer housing.

Within the heated section, coolant flowed in the channels between pairs of adjacent concentric tubes. Spacer ribs divided each flow channel into four subchannels. Figure 2 shows the cross-sectional profile of the SPRIHTE rig. As this figure illustrates, the rig contained two heated tubes and two unheated tubes, which correspond to the fuel and target tubes of a fuel assembly. The rig differed from an actual fuel assembly, however, in that the there was no outer housing. The purge channel between the outer target tube and this outer housing was replaced by two external bypass tubes located on opposite sides of the heated section, as shown by Figure 1.

The test rig also differed from a fuel assembly in that only the middle two tubes of the test rig, corresponding to the inner and outer fuel tubes of the reactor assembly, were heated. In a fuel assembly, both the fuel and the target tubes generate heat. The outer heater tube of the test rig received 60% of the electrical power, and the inner heater tube received 40%. The heater tubes were constructed to give an axial power profile prototypic of a fuel assembly. The maximum power was located about three-quarters of the distance from the top of the heated section and was 1.43 times the average power.

As mentioned previously, the test rig was prototypic of a Savannah River reactor fuel assembly in that it had the same dimensions. Table 1 lists the dimensions of the test rig and compares the measured cross-sectional diameters rig with the design diameters of a Savannah River fuel assembly.

Overall flow rates to the SPRIHTE rig were measured using ultrasonic and turbine flow meters; the ultrasonic flow meters measured high flow rates and the turbine flow meters measured low flow rates. Individual channel and subchannel flow rates were not metered. The rig was fully instrumented to measure subchannel coolant and heater wall temperatures. Wall and subchannel coolant temperatures were measured using thermocouples; inlet and outlet fluid temperatures were measured using resistance temperature devices (RTD's). Inlet and outlet pressures also were measured. Measurement uncertainties were 2-3% for the ultrasonic flow meters, about 2% for the turbine flow meters, 1.0 K or less for the thermocouples, 0.5 K for the RTD's, and 1000 Pa or less for the pressure gauges [5]. In addition, the ultrasonic flow meter measurements were biased about 1% low, and the heater wall temperature measurements were biased about 1 K low [5]. No corrections were made to compensate for these biases.

During the tests, the flow rate and the inlet temperature were held constant, and the power was increased in increments until a thermal excursion was detected by wall thermocouples. A constant downward flow through the test section was maintained by a centrifugal pump with a high impedance. A standpipe connected to the test rig discharge kept pressures constant. The discharge was located just above the inlet plenum and was open to the atmosphere. Because pressure losses in the discharge line were small, it was assumed that the outlet from the heated section was under the static head of the discharge line.

Prior to thermal excursion, fluid thermocouple measurements indicated that there was unstable flow and flow reversal (upflow) in one of the outer subchannels. The thermal excursions always occurred in the outer channel. Unstable flow was detected by means of fluctuations of about 5 K in the effluent temperature. Flow reversal was said to occur when the inlet temperature exceeded any downstream temperature by 20 K or more. Finally, thermal excursions began when the maximum outer heater wall temperature reached 450 K. Power was shut off at this point to prevent damage to the rig.

Tests were conducted at flow rates of 0.000323, 0.000647, and 0.00097 m³/s and at inlet temperatures of 298 K and 313 K. Only the 0.000647 and 0.00097 m³/s tests were analyzed, since these flow rates were within the flow range at which the limit for the ECS addition phase of the LOPA was set [3]. Table 2 lists estimated individual channel flow rates, flow velocities, and Reynolds numbers for these tests.

Description and Evaluation of the Computational Model

The SPRIHTE tests were modeled using FLOPA, a finite difference thermal-hydraulic code developed at the Savannah River Site [6]. This code was an adaptation of another Savannah River code, FLOWTRAN, which was written to compute limits for the Loss of Coolant Accident [7]. Both codes combined a three-dimensional finite difference heat conduction model for the fuel assembly tubes with a one-dimensional donor cell model for flow and heat transfer in each subchannel. From comparisons with known analytical solutions, the codes' heat conduction calculations were accurate within about 0.6% [7]. Fluid temperatures calculated by the donor cell model were offset by one-half cell length. The heated length of the SPRIHTE test rig was divided into 40 axial cells for the calculations in this study. Thus, for a typical temperature increase of 60 K, the calculated temperatures were low by about 0.75 K. No correction was made for this offset.

The primary sources of uncertainty in the model calculations were fluid heat transfer coefficients and friction and form loss factors for subchannel flow. Fluid heat transfer was modeled using a modified Sieder-Tate forced convection correlation [7]:

$$\frac{hD_h}{k} = 0.023\left(\frac{D_h G\rho}{\mu}\right)^{0.8}\left(\frac{c_p\mu}{k}\right)^{1/3} \tag{3}$$

Friction and form loss factors were obtained from constant temperature fuel assembly hydraulic test results. Differences between nominal fuel assembly and SPRIHTE rig tube diameters were small and were therefore ignored. It was assumed that the surface roughness of the test rig tubes was the same as that of reactor assemblies and that the heated section inlet and bottom end fittings were prototypic. The use of prototypic fuel assembly dimensions and friction and form loss factors from standard fuel assembly hydraulic tests was justified through comparisons of measured and calculated fluid and wall temperatures under stable flow conditions. These comparisons showed that the use of nominal dimensions and loss factors did not have a significant adverse effect on the ability of the FLOPA code to predict these temperatures. Neither heat transfer nor fluid flow models accounted for the presence of localized boiling where surface temperatures were higher than average, for instance, opposite spacer ribs.

The effect of thermocouple insertions on the flow in the inner and outer channels was assumed to be negligible, and corrections to fluid thermocouple measurements to account for fluid temperature gradients were not considered. Corrections to wall thermocouple measurements to account for thermal gradients in the heater tubes also were ignored. The wall thermocouples were centered within the heated walls. Subsequent calculations using the new limit criterion for the tests showed that the difference between the center wall and surface temperatures was 0.3 K at limit conditions. This difference was judged to be insignificant.

Finally, in calculations to determine a limit criterion, the test rig was modeled as a series of concentric annuli. Differences among subchannel fluid temperature measurements, particularly for the outer channel, indicated that the test rig cylinders may have been

eccentric. However, no credit was taken for this apparent eccentricity in the limit criterion analysis, since the eccentricity was not measured under heated conditions.

To determine the effect of eccentricity, three-dimensional, eccentric FLOPA models were used. Three models were created. In the first, designated Case 1 for ease of reference, the eccentricity of the outer channel was set to match the calculated difference between the hottest and coldest subchannel in the outer channel with the measured difference. In the second, designated Case 2, the eccentricity of the outer channel was set at its maximum value allowed by the rib tip clearance. Finally, in Case 3, a model was created in which the eccentricities in all three flow channels were set at the maximum values allowed by rib tip clearances. The eccentric channels were aligned in the same radial direction to maximize differences in subchannel heat transfer rates. Case 3 was used in LOPA limits calculations.

To verify that the FLOPA calculations accurately modeled flow and heat transfer in the test rig, calculated and measured values for subchannel fluid and heated wall temperatures were compared. In these comparisons, the Case 1 eccentricity model was used. A separate match was performed for a heated stable flow test at each test condition. Figure 3 compares typical fluid temperature profiles for the outer channel under stable flow conditions. This figure shows that FLOPA modeled flow and heat transfer to the coolant within a range of about 5 K. Figure 4 compares outer heater wall temperature profiles for the stable flow test condition at 0.00097 m^3/s and 313 K inlet. Again, the FLOPA model predicted measured temperatures within about 5 K. Figure 5 compares these wall temperatures at a higher power, where flow became unstable in the outer channel. In this case, measured wall temperatures for two of the outer subchannels are higher than the calculated temperatures, indicating that flow was diverted to the inner two channels.

Selection of a Limit Criterion

To bound the results of the tests, a criterion that the wall temperature not exceed the fluid saturation temperature was used. This wall saturation temperature criterion ensures that there is no boiling along the heated walls and, therefore, a thermal excursion cannot occur. A multiplier was added to account for differences between measured and calculated subchannel flow and heat transfer rates up to the point where unstable flow and possible flow reversal occur (see the discussion of wall temperature distributions in the preceding section). The limiting fluid temperature, in (degrees K - 273), is the product of this multiplier and the saturation temperature in (degrees K - 273).

Measured and computed maximum wall temperatures were compared to verify that FLOPA could accurately calculate the wall saturation temperature criterion. The maximum temperatures for these comparisons were located on the outer wall of the outer heater (the inner wall of the outer flow channel). Figure 6 illustrates these comparisons for the concentric flow model and for Cases 1, 2, and 3 eccentricity models. The Case 3 model was used to calculate LOPA limits. For Case 1, the FLOPA model accurately predicted the maximum wall temperature at low powers under steady flow conditions, but underestimated the maximum temperatures by as much as 10 K at higher powers.

Limits were computed for the concentric flow model and for Cases 1 and 2. For the eccentric cases at 0.000646 m^3/s, the FLOPA code predicted that flow reversal would occur in one subchannel of the outer channel. FLOPA did not predict that flow reversal would occur prior to measured thermal excursion conditions at 0.00097 m^3/s.

Figure 7 illustrates the comparisons between measured conditions and calculated limits. The powers where unstable flow and flow reversal were first detected in the outer channel are noted, as are the powers where the maximum measured wall temperature first exceeded the fluid saturation temperature and where thermal excursions took place. The onsets of unstable flow, flow reversal, and thermal excursion occurred somewhere between these power levels and the next lower powers. The powers at which the maximum wall temperature equaled the saturation temperature were determined by linear interpolation of measurements at different test conditions.

Figure 7 compares these measured conditions with calculated limits using the wall saturation temperature criterion with different multipliers and with the previously determined Stanton number limit for a LOPA (see Equation 2). Comparisons are made for the wall saturation temperature criterion with the concentric and Case 1 and 2 eccentric flow models.

Linear interpolations were performed to determine multipliers to match measured and calculated powers at which the maximum wall temperature first exceeded the saturation temperature. The powers for these interpolations were calculated based on both the concentric flow channel model and the Case 1 eccentric flow model.

The multiplier for the wall saturation temperature criterion was based on the calculated results for concentric channels. Table 3 lists the results of these calculations. A wall saturation temperature criterion multiplier of 0.885 was recommended for calculating LOPA ECS addition phase limits. For the four tests analyzed in this report, this is the average value of the multiplier that matches measured and calculated powers at which the maximum wall temperature equals the saturation temperature. The margin between the limiting power for this value of the multiplier and the power at thermal excursion is between 15% and 20%.

Table 4 gives the effect of the wall saturation temperature multiplier on the limit for the ECS addition phase of the LOPA. According to the results in this table, a multiplier of 0.885 would yield a limiting power that is 37% of the limiting power for previous long-term reactor operations.

Transition between High and Low Flow Rate Criterion

The wall saturation temperature criterion is applicable only at low flow rates, where the tests have demonstrated that buoyancy-induced flow reversal can occur prior to the onset of flow instability. A Stanton number criterion was retained for use at higher flow rates, where buoyancy effects are not significant. The wall saturation temperature criterion was restricted to Peclet numbers below 70,000, where the Peclet number is defined by

$$Pe = \frac{D_h c_p G}{k} \tag{4}$$

This value corresponds to the lowest Peclet number tested in benchmarking the LOCA-FI Stanton number criterion (St = 0.00455) [8] and is considerably above the value where buoyancy effects are significant.

The structure of the FLOPA limits code made it easier to specify when to apply the wall saturation temperature criterion in terms of a transient time instead of a Peclet number. Figure 8 depicts variations in the Peclet numbers in the limiting subchannel (located outside the outer fuel tube of the fuel assembly) for a typical LOPA transient. As shown

in this figure, the wall saturation temperature criterion takes effect 344 seconds after the start of the LOPA transient, when the DC pump motors flood and the DC pumps begin to coast down. The Peclet number at this time is approximately 70,000.

Conclusion

Based on the results of the SPRIHTE rig tests, a wall saturation temperature criterion was recommended for calculating the limit for the ECS addition phase of the LOPA. An analysis of preliminary test results was used to set this limit criterion. This analysis shows that the maximum wall temperature inside the assembly should not exceed 0.878 times the local fluid saturation temperature in degrees C. Use of the criterion with this multiplier set the LOPA core power limit at 37% of the limiting power for previous long-term reactor operations.

References

[1] B. J. Hardy and A. M. White, "A Probabilistic Method for Determining Effluent Temperature Limits for Flow Instability in SRS Reactors (U)," Westinghouse Savannah River Company Report, WSRC-TM-90-5 (DPSTM-160) (1990).

[2] P. Saha and N. Zuber, "Point of Net Vapor Generation and Vapor Void Fraction in Subcooled Boiling," Proceedings, 5th International Heat Transfer Conference, Tokyo, Japan, Vol. 4 (1974).

[3] P. K. Paul and K. L. Barbour, "DEGB LOPA Limit Recommendation for the K-14.1 Subcycle," Westinghouse Savannah River Company Report, WSRC-RP-91-444, Rev. 1 (1992).

[4] B. S. Johnston, "Limits for Stable Downward Flow in a Single Heated Annulus at LOPA Conditions," Westinghouse Savannah River Company Report, NES-ETH-910190 (1991).

[5] H. N. Guerrero and C. M. Hart, "SPRIHTE Prototypic Assembly LOPA Test Data Report," Westinghouse Savannah River Company Report, WSRC-TR-93-012 (1993).

[6] S. E. Aleman, "Documentation of FLOWTRAN for Loss of Pumping Accident Analyses (FLOPA)," Westinghouse Savannah River Company Report, NES-CDG-910133 (1991).

[7] S. E. Aleman, M. V. Gregory, L. L. Hamm, L. D. Koffman, R. E. Pevey, W. H. Reed, and F. G. Smith, "FLOWTRAN: An Algorithm for Describing the Thermal-Hydraulic Behavior of SRP Assemblies (U)," Westinghouse Savannah River Company Report, DPSTM-140, Rev. 0 (1989).

[8] J. A. Block, C. J. Crowley, F. X. Dolan, R. G. Sam, and B. H. Stoedefalke, "Nucleate Boiling Pressure Drop in an Annulus," Creare, Inc., Technical Note, TN-499, Vol. 1 (1990).

Nomenclature

A_x cross-sectional flow area
c_p fluid heat capacity
D_h hydraulic diameter of coolant channel
G coolant mass flux
h wall heat transfer coefficient
k fluid thermal conductivity
Pe Peclet number
q'' surface heat flux
St Stanton number
T_{bulk} bulk coolant temperature
T_{sat} fluid saturation temperature
μ fluid viscosity
ρ fluid density

**Table 1. Comparison of Savannah River Fuel Assembly Design
and SPRIHTE Rig As-Built Dimensions**

Dimension	Fuel Assembly Design	SPRIHTE Min.	SPRIHTE Max.
Inner Target OD	0.04039	0.04039	0.04041
Inner Target Rib Circle	0.04989	0.04983	0.04999
Inner Heater ID	0.05067	0.05057	0.05065
Inner Heater OD	0.05977	0.05977	0.05982
Inner Heater Rib Circle	0.07272	0.07264	0.07282
Outer Heater ID	0.07346	0.07353	0.07363
Outer Heater OD	0.08128	0.08136	0.08141
Outer Target Rib Circle	0.08204	0.08197	0.08242
Outer Target ID	0.08992	0.08954	0.08999

Distance from Inlet Plenum to Top of Fuel Assembly	1.72
SPRIHTE Inner Heater Heated Length	3.76
SPRIHTE Outer Heater Heated Length	3.91
Fuel Assembly Design Overall Length	3.84
Fuel Assembly Design Heated Length	3.78

All dimensions are in m.

Table 2. Flow Conditions for Tests

Channel	Flow Rate (m³/s)	Velocity (m/s)	Reynolds Number
Total	0.000647		
Inner	0.000134	0.19	3700
Middle	0.000308	0.22	6700
Outer	0.000205	0.18	4200
Total	0.00097		
Inner	0.000201	0.28	5500
Middle	0.000462	0.33	10000
Outer	0.000307	0.27	6300

Table 3. Measured Flow Reversal and Flow Instability Conditions

Flow Rate (m³/s)	Inlet Temperature (K)	Condition	Power (W)
0.000647	298	Flow Reversal	106,800
		Wall Temp. = Sat'n Temp.*	130,800
		Thermal Excursion	160,600
0.000647	313	Unstable Flow	74,100
		Flow Reversal	80,700
		Wall Temp. = Sat'n Temp.*	92,400
		Thermal Excursion	127,100
0.00097	298	Unstable Flow	183,200
		Flow Reversal	197,300
		Wall Temp. = Sat'n Temp.*	199,100
		Thermal Excursion	231,400
0.00097	313	Unstable Flow	132,200
		Flow Reversal	151,800
		Wall Temp. = Sat'n Temp.*	164,100
		Thermal Excursion	188,200

*This power was estimated by linear interpolation of maximum measured wall temperatures at different test conditions.

Table 4. Comparison of Calculated and Measured Wall Saturation Temperatures

The wall saturation temperature criterion multipliers match measured and calculated powers at which the maximum wall temperatures first exceeded saturation temperatures, based on corrected wall temperature measurements.

| Flow Rate (m³/s)	Inlet Temperature (K)	Power when Max. Wall Temp. = Satn. Temp. (W)	Wall Saturation Temp. Criterion Multiplier
0.000647	298	130,800	0.881
0.000647	313	92,400	0.832
0.00097	298	199,100	0.905
0.00097	313	164,100	0.923
			0.885 = average
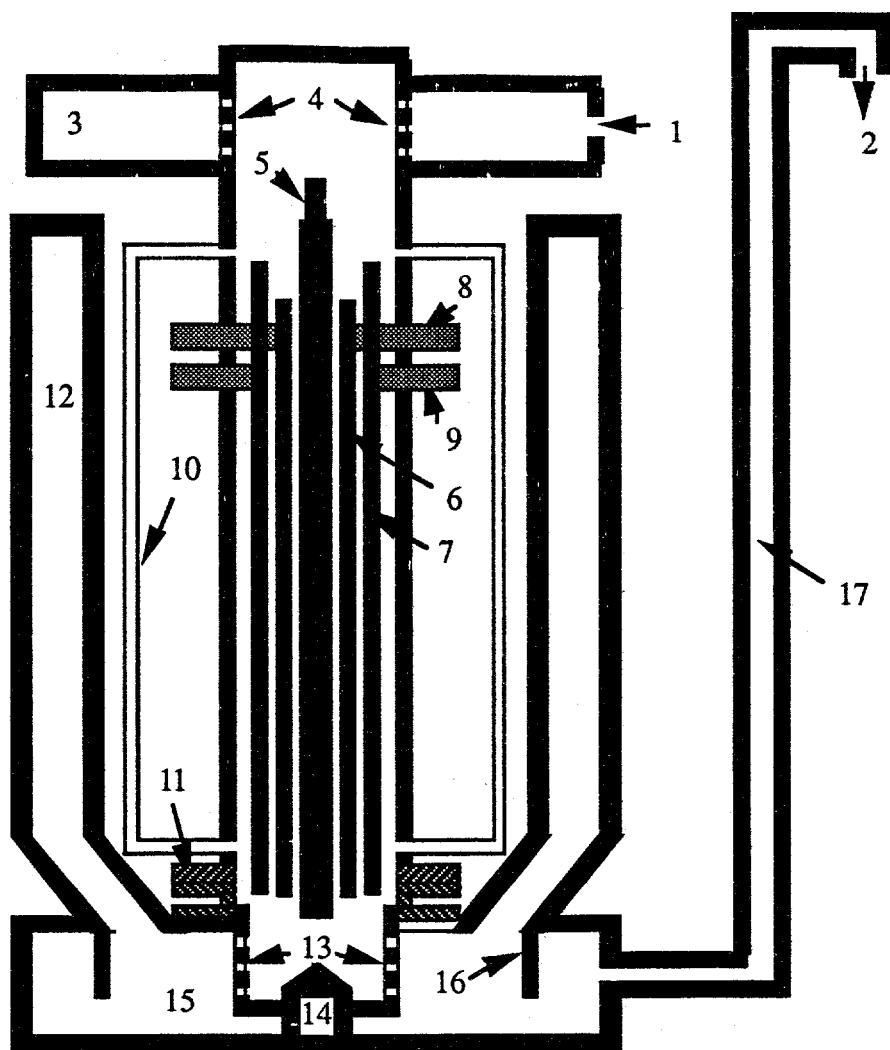
Figure 1. Test Apparatus Schematic. A key to figure captions follows.

1. Water Inlet from Flow Meters
2. Outlet to Catch Basin, Pump, and Heat Exchanger
3. Inlet Plenum
4. Perforated Tube Inlet to Heated Section
5. Center Pin (corresponds to Inner Target Tube)
6. Inner Heated Annulus
7. Outer Heated Annulus
8. Electrical Bus for Inner Heated Annulus
9. Electrical Bus for Outer Heated Annulus
10. Outer Bypass Tubes (one each side)
11. Bottom Flange
12. Unvented Air-Water Separators (one each side)
13. Perforated Tube Outlet from Heated Section
14. Monitor Pin
15. Outlet Plenum
16. Baffles
17. Outlet Standpipe
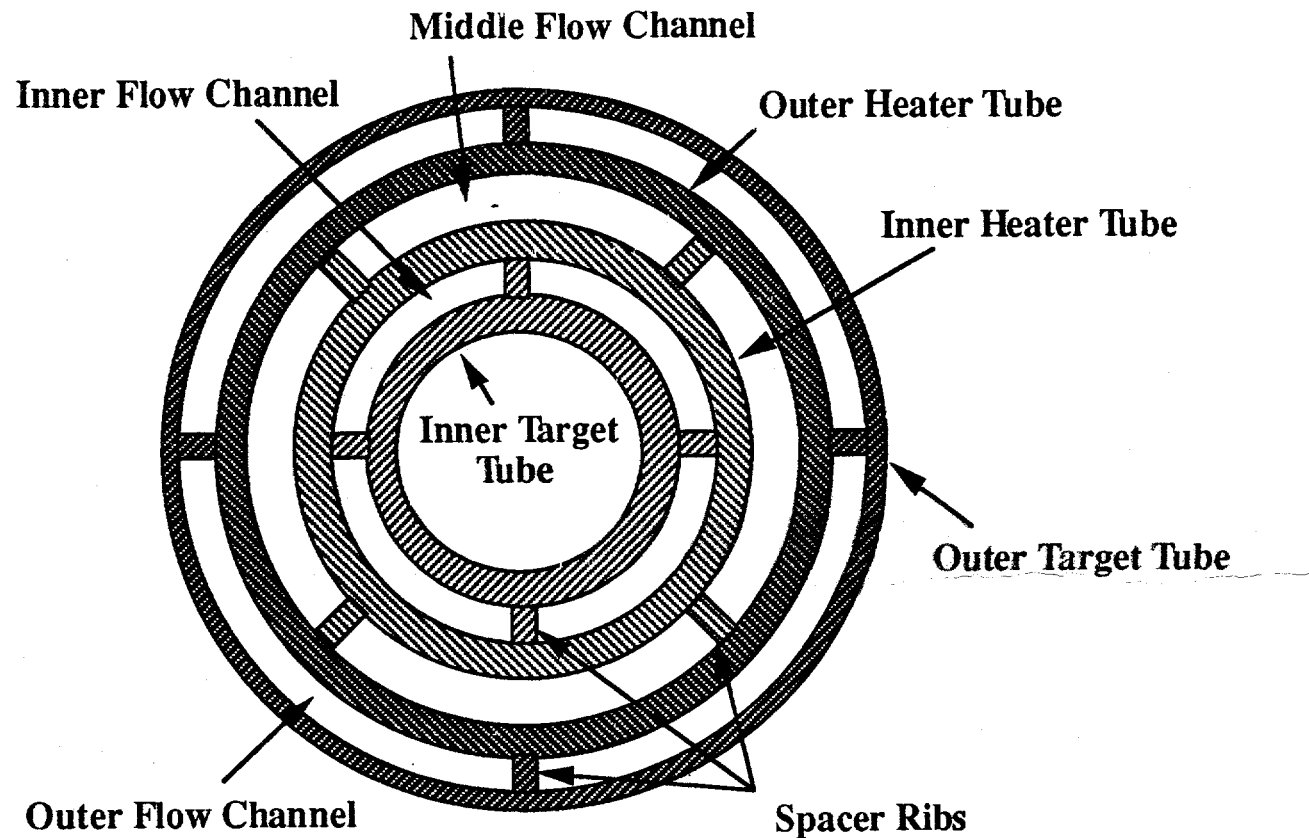
Figure 2. Cross-Sectional View of SPRIHTE Test Rig
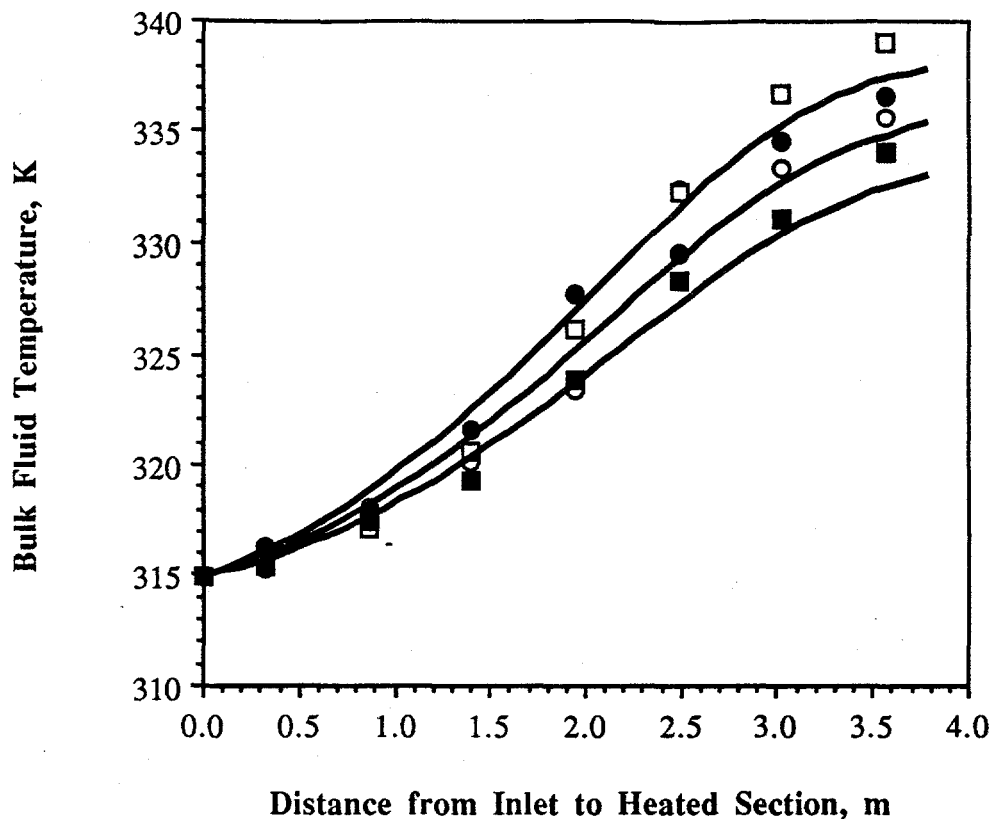
Figure 3. Comparison of Measured and Calculated Subchannel Fluid Temperatures for the Outer Channel at 0.00097 m³/s, 40°C Inlet, 78,000 W

Symbols represent bulk fluid temperature measurements for the four outer subchannels. Lines represent calculated fluid temperatures for these four subchannels. (Calculated temperature profiles for two or more subchannels may coincide because of assumed symmetries in the model.) No correspondence between calculated temperature profiles and specific subchannel measurements is implied.
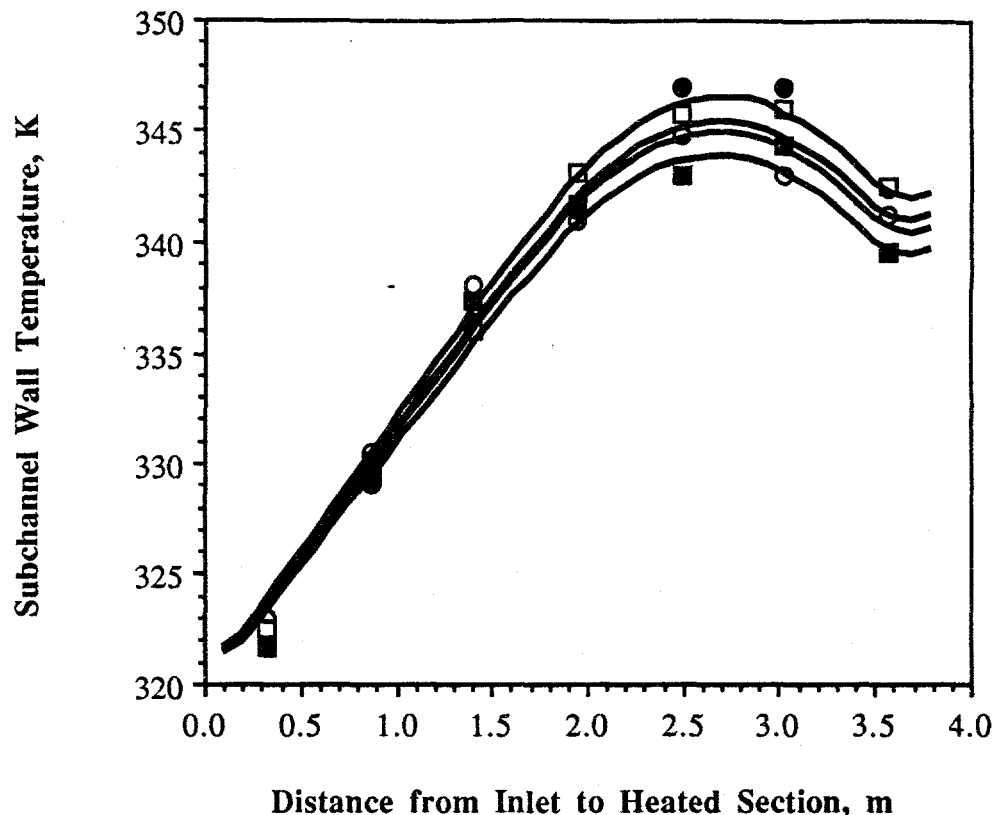
Figure 4. Comparison of Measured and Calculated Outer Heater Wall Temperatures
at 0.00097 m³/s, 40°C Inlet, 78,000 W

Symbols represent outer heater wall temperature measurements for the four subchannels.
Lines represent calculated outer heater wall temperatures for the four subchannels.
(Calculated temperature profiles for two or more subchannels may coincide because of
assumed symmetries in the model.) No correspondence between calculated temperature
profiles and specific subchannel measurements is implied.
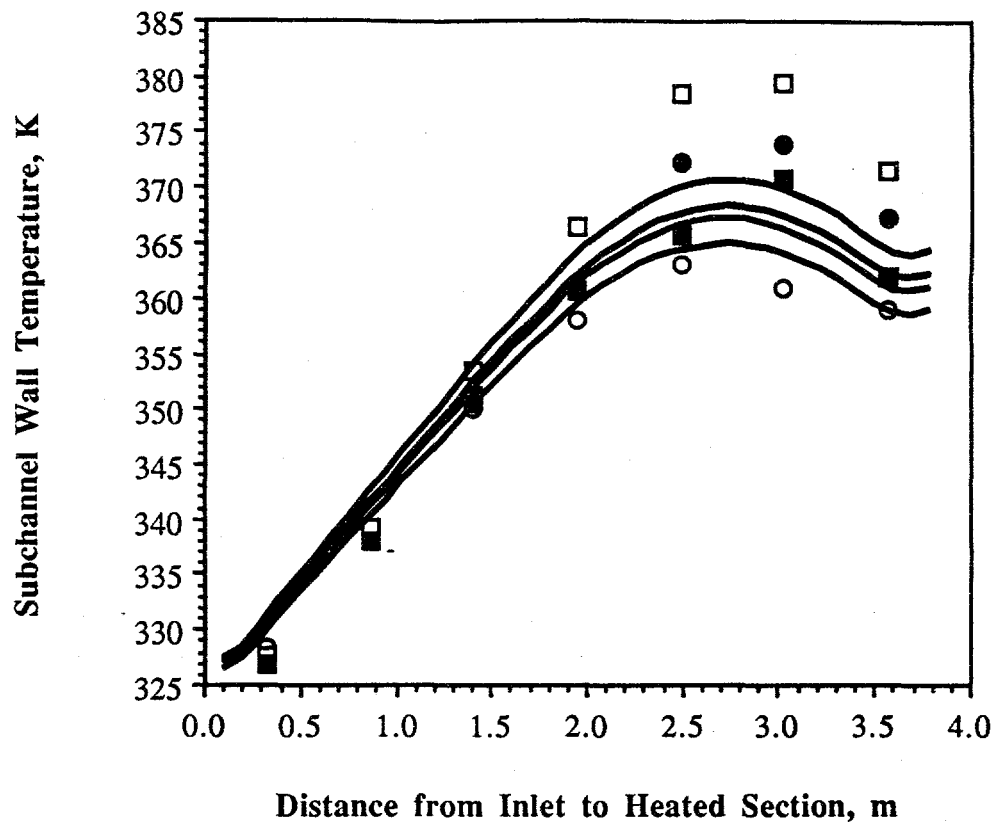
Figure 5. Comparison of Measured and Calculated Outer Heater Wall Temperatures
at 0.00097 m³/s, 313 K Inlet, 142,000 W

Symbols represent outer heater wall temperature measurements for the four subchannels.
Lines represent calculated outer heater wall temperatures for the four subchannels.
(Calculated temperature profiles for two or more subchannels may coincide because of
assumed symmetries in the model.) No correspondence between calculated temperature
profiles and specific subchannel measurements is implied.
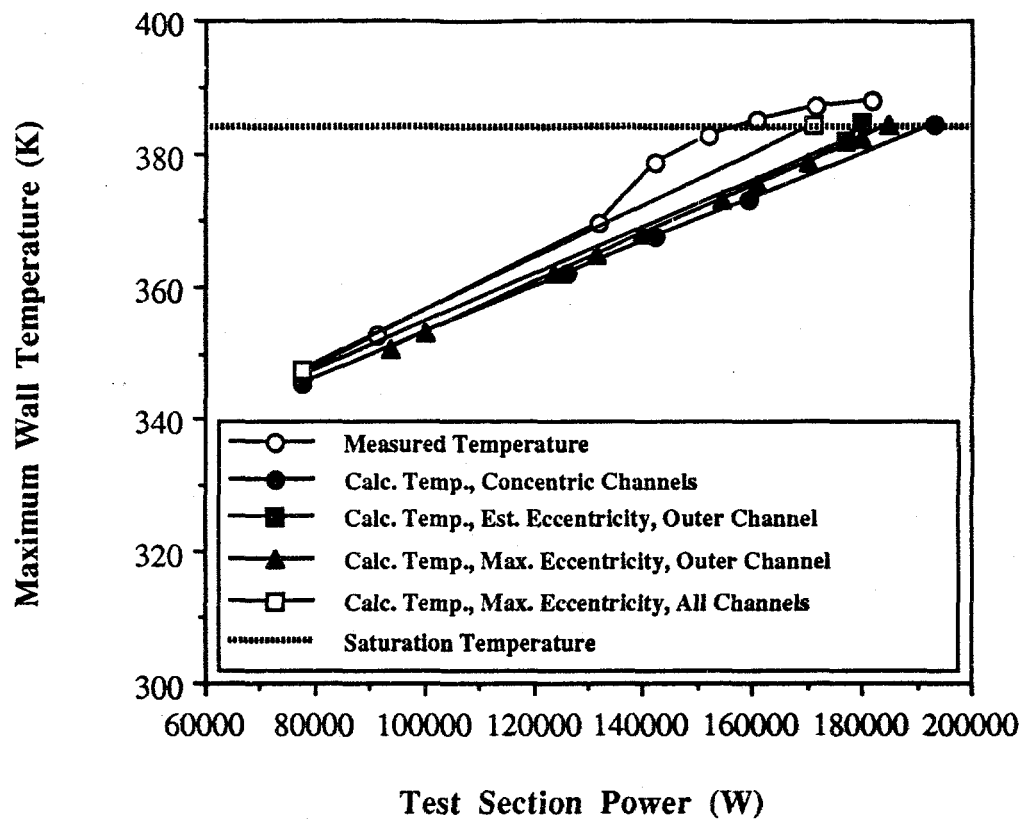
Figure 6. Comparison of Measured and Calculated Maximum Wall Temperatures
for the SPRIHTE Tests at 0.00097 m³/s and 313 K Inlet.
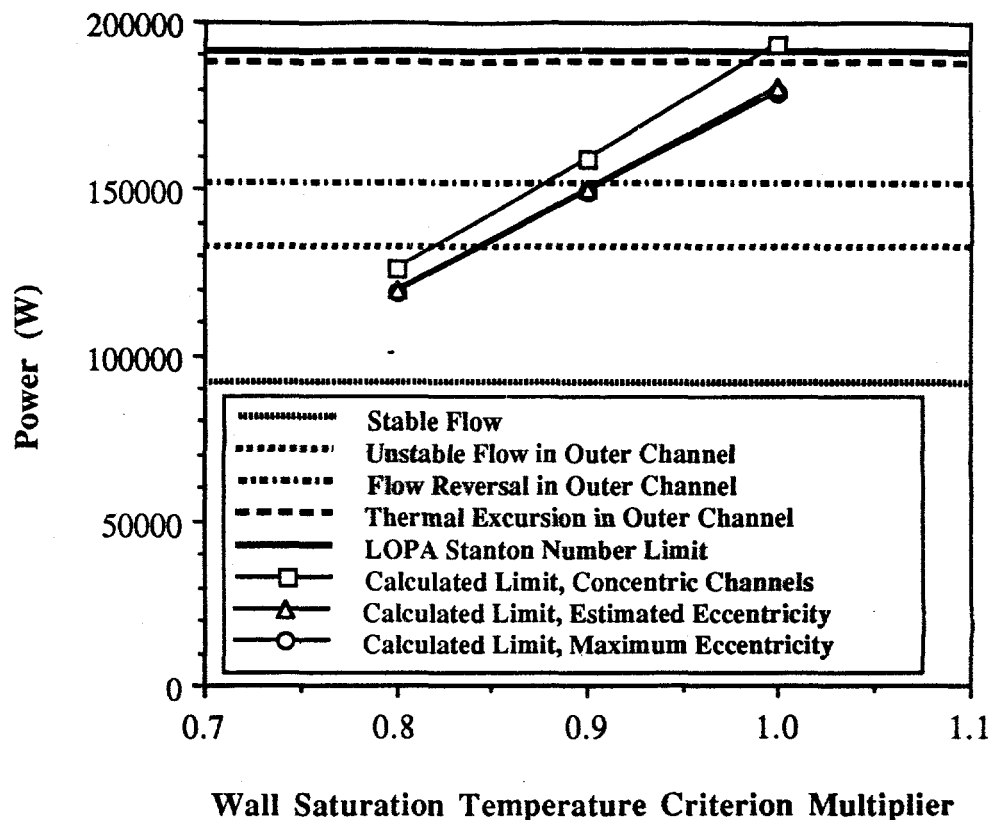
Figure 7. Comparison of Wall Saturation Temperature Criterion Limits with Measured
Conditions for the SPRIHTE Tests at 0.00097 m³/s and 313 K Inlet.
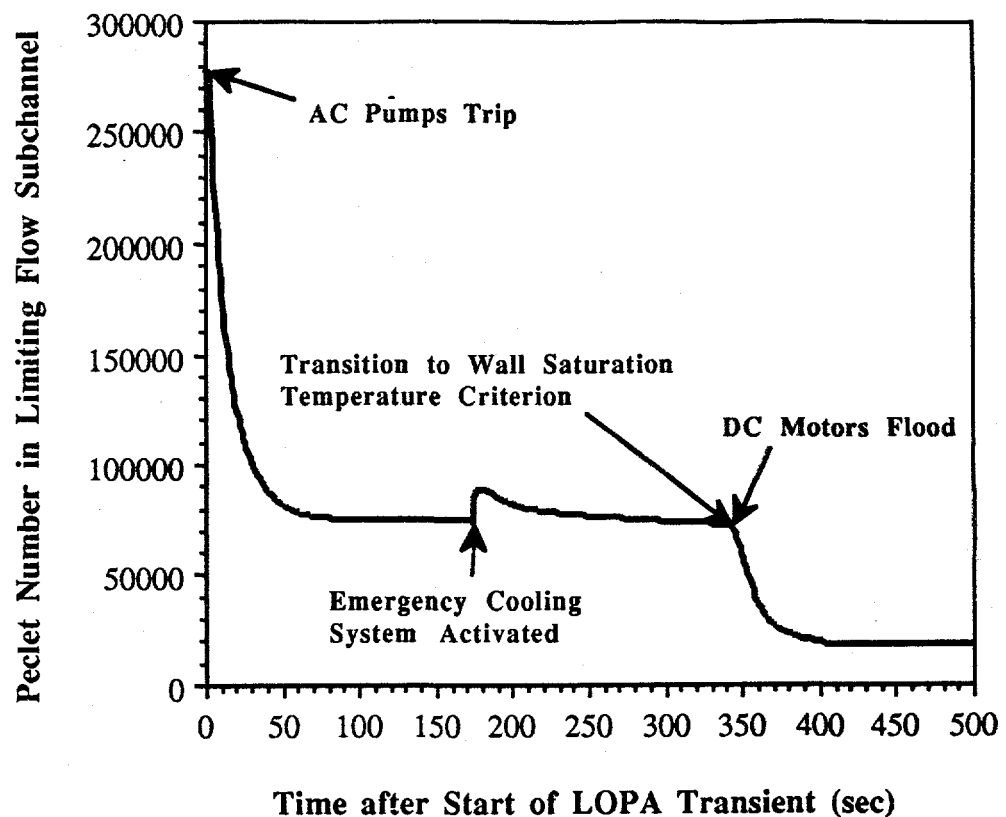
Figure 8. Variation of Peclet Numbers in the Limiting Subchannel during the LOPA Transient